Proceedings of the 2019 Design of Medical Devices Conference
DMD2019
April 15, 16-18, 2019, Minneapolis, MN, USA

DMD2019-3300

AUTOMATED MANUFACTURING OF FIBER-REINFORCED ELASTOMERIC ENCLOSURES FOR PATIENT SPECIFIC CATHETER ROBOTS

Ben Hamlen[1], Gillian McDonald, Mark Gilbertson, Daniel Ng, Timothy Kowalewski
University of Minnesota – Twin Cities
Minneapolis, Minnesota, United States

ABSTRACT

"No-option" patients have vasculature too tortuous for existing catheters to navigate. To treat these patients, new catheter technologies are needed that are easy to actuate and can be customized for each patient. We propose using fiber-reinforced elastomeric enclosures (FREEs), which have been shown to be capable of performing screwing, spiraling, twisting, extending, and other motions when the fiber wrap angles are adjusted. Here, we present and validate an automated system capable of manufacturing FREEs with wrap angles from 0-90 degrees. The prescribed fiber angles were within 5 percent error when manufactured.

Keywords: catheters, patient-specific manufacturing

INTRODUCTION AND BACKGROUND

Heart disease is the leading cause of death in the United States [1]. Stents – the most popular method of treatment for the disease – provide viable treatment, but clinicians we interviewed around Minneapolis estimate stents are unsuitable for use on 2-5% of cardiovascular patients because of their tortuous vasculature. These patients are deemed "no-option patients." One possible solution to this problem is to replace traditional catheters with soft robots that gently pull themselves through veins and arteries to reach the site of the occlusion. The soft construction materials used and their ability to conform to their surroundings make soft robots ideal for in-vivo use. Locomotion is achieved by pressurizing and depressurizing saline held inside FREEs [2], referred to here as "actuators". The use of fluid-filled FREEs in this work was inspired by the work of Bishop-Moser Et al. [3]. Two actuators expand to form helices to grip the outer walls of the passage being navigated, and one central actuator extends to push the robot forward (Fig. 1). However, the method in [2] may need to be tuned to specific patients, requiring a custom soft robot design for their specific anatomy. Custom catheter robots could also help address the problem of wasted medical supplies. Every year hospitals throw out billions of dollars' worth of unopened or opened and never-used supplies. This waste comes, in part, from overproduction and accidental use of improperly sized devices [4]. Patient-specific robots address this waste by enabling hospitals to produce a custom robot only when one is needed. The end-goal of this research is to enable use of patient anatomy data (from an MRI or similar scan) and have machines in the hospital make the robot that day.

The aim of the work presented here was to design a more automated manufacturing setup and methods to construct FREEs and evaluate their construction. Specifically, we determine the capability of our system to i) deposit fibers at desired angles as needed for a patient-specific design and ii) determine the accuracy of the deposited fibers' wrap angles using manual and computer vision means.

1 Methods

1.1 Construction

The manufacturing setup used a Prazi lathe, stripped of its motors and electronics (Fig. 2). A belt drive system was designed to control both the central rotating axis of the lathe (the "Rotation Stage") and the worm gear driving the carriage (the "Linear Stage"). To drive this belt system, direct drive DC Motors (Maxon) were attached to laser-cut MXL pulleys and controlled with a Teensy 3.5 microcontroller and Pololu Dual VNH3SP30 motor driver. This gives a mechanical advantage of 27:1 in the belt pulley system. Encoders were used to measure the position of both stages throughout their motion. The rotation stage utilized a 22-bit absolute inductive encoder (NC-3-150-221001-SPI1-RFC4-5-AN Zettlex Systems, Inc). The linear stage used a transmissive optical linear encoder with 3000 counts per inch (CPI) from US Digital (EM2) (Fig. 2).

[1] Contact author: hamle012@umn.edu

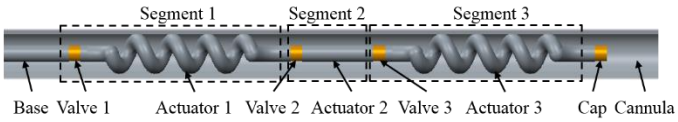

FIGURE 1: Rendering of envisioned catheter robot.

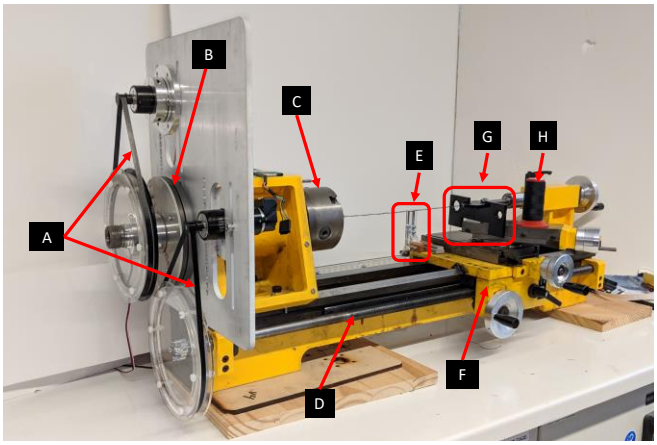

FIGURE 2: Top: Experimental setup of modified lathe; A: Zero Backlash MXL Belt Drive, B: 22-bit Absolute Rotary Encoder, C: Rotation Stage, D: Worm Gear, E: Linear Encoder, F: Linear Stage, G: Thread Guide, H: Thread Spool.

A thread spool holder and guide were designed for the linear stage. The thread was fed through a hole in the guide and then attached to the actuator being wrapped. This was typically accomplished by adhering the string to the tube with tape and then closing the lathe's chuck teeth on top of the tape.

1.2 Velocity Controller

The desired wrap angle was achieved by relating the linear stage's velocity (v_{lin}) to the circumferential velocity of the outer surface (v_{rot}) of the actuator being wrapped by

$$v_{rot} = v_{lin} \tan(\theta_{wrap}) \quad (1)$$

The linear stage was set to run at a constant 4.5 mm/s.

The circumferential velocity of the outer surface of the actuator being wrapped was calculated by

$$v_{rot} = \frac{1}{2^{22}} \pi v D \quad (2)$$

Where v is the velocity of the rotation stage measured in counts per second from the absolute rotational encoder, D is the outer diameter (OD) of the actuator being wrapped, and 2^{22} is the number of counts per full revolution given by the absolute rotational encoder.

v_{rot} was controlled with a PID controller running at 1kHz. Zeigler-Nichols and various step inputs were used to tune the gains, resulting in $K_p = 10, K_i = 12.5, and\ K_d = 0.09$.

1.3 Testing and Validation

The performance of the velocity controller was characterized by wrapping 20º, 45º, and 80º wrap angles, as the range of angles for actuator manufacturing is expected to be 20º - 80º. Per Equation 1, v_{lin} of 1.64, 4.5 and 25.52 mm/s correspond to wrap angles of 20º, 45º, and 80º, respectively. Ten trials at the aforementioned v_{lin}, each trial making step changes from zero to the specified velocity, were conducted. The average velocity response over the ten trials for each v_{lin} was calculated. MATLAB's curve fitting toolbox was used to fit the average velocity response data for each target wrap angle to determine a 95% rise time (time from step to less than 5% error).

Generated wrap angles were qualitatively examined by overlaying a line at the desired wrap angle on a photo of the wrapped cylinder (Fig. 5). This was accomplished by turning on the "rule of thirds" [5] grid guide on a Pixel 2 XL phone camera. One of those lines was aligned with the edge of the actuator, providing a ground truth for horizontal alignment of the actuator in the photo frame. The photo was then digitally cropped to align the actuator with the center of the image. A horizontal line was drawn from the left center of the image to the right center (white dashed lines in Fig. 5). That line was duplicated, rotated in Microsoft Word to the specified wrap angle, and changed to solid red.

Accuracy of wrap angles was quantitatively examined using OpenCV in Python (opencv-contrib-python library). A region of interest (ROI) was extracted from the center of the image. The ROI top and bottom bounds were approximately 20% smaller than the visible edge of the catheter and horizontal extents were clipped to where the visible fiber started to deviate from a straight line. A sample ROI around a single fiber is shown in Figure 3. To extract fiber angle, the following steps were taken:

1. Median blur of 5 pixels & conversion to grayscale
2. Binary threshold at 50%
3. Canny edge extraction
4. Hough Transform line extraction (HoughLines) with 1-degree accuracy and threshold selected by decreasing from 100 until more than 1 line was returned. The angle of the two best lines was extracted from Hough parameters and averaged and reported as the angle of the thread derived from computer vision.

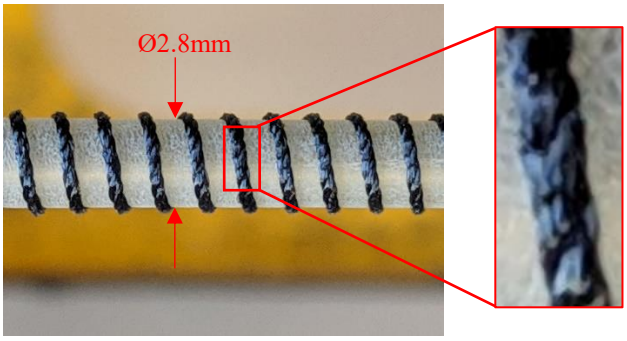

FIGURE 3: Acquired image of 80° wrap angle, 2.8mm OD shaft; Insert: sample extracted region of interest (ROI) for computer vision-based wrap angle measurement.

2 Results

Results for the control system are given in Figure 4 and Table 1.

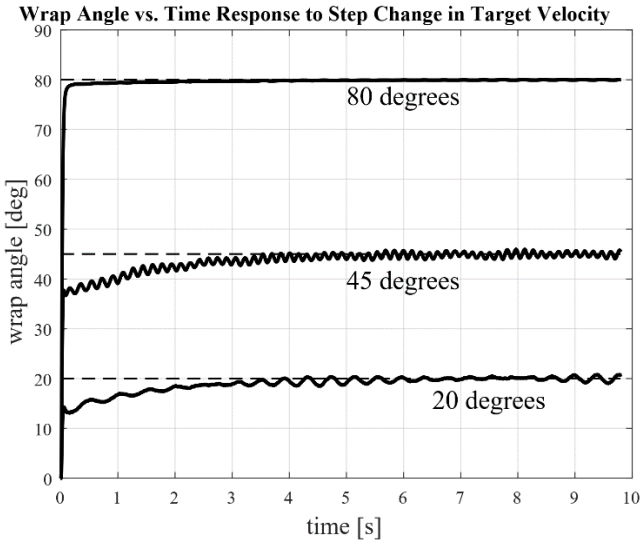

FIGURE 4: Instantaneous wrap angle produced by controller in response to step inputs of 1.64, 4.5 and 25.52 mm/s (20, 45, and 80 deg. wrap angles, respectively). Dashed lines are desired wrap angles, solid lines are actual wrap angles.

MATLAB's curve fitting toolbox minimized error with a double exponential function as shown in Equations 3-5 below.

$$v_{rot,20} = 1.64 - 1.42e^{\frac{-t}{.017}} - 0.58e^{\frac{-t}{1.66}} \quad (3)$$

$$v_{rot,45} = 4.5 - 4.34e^{\frac{-t}{0.02}} - 1.17e^{\frac{-t}{1.79}} \quad (4)$$

$$v_{rot,80} = 25.54 - 28.75e^{\frac{-t}{0.05}} - 2.16e^{\frac{-t}{2.77}} \quad (5)$$

These fits were used to calculate the 95% rise time for each wrap angle (Table 1).

The length of the actuator with wrap angle error greater than 5% was calculated by

$$L_{innacurate} = 4.5t_{95\%} \quad (6)$$

Where 4.5 is the constant velocity of the linear stage (mm/s) and $t_{95\%}$ is the 95% rise time (s) for that wrap angle (Table 1).

Wrap Angle *(degrees)*	$t_{95\%}$ *(seconds)*	$L_{innacurate}$ *(mm)*
20	3.30	14.85
45	3.00	13.50
80	1.43	6.435

TABLE 1: Time from 0 to <5% error from set point (95% rise time) and length of actuator with inaccurate wrap angles for 20, 45, and 80-degree wrap angles.

Figures 5 and 6 show the results of the manual and computer-vision based accuracy measurements, respectively. Figure 7 shows two actuators constructed with the automated process using pre-programmed wrap angles.

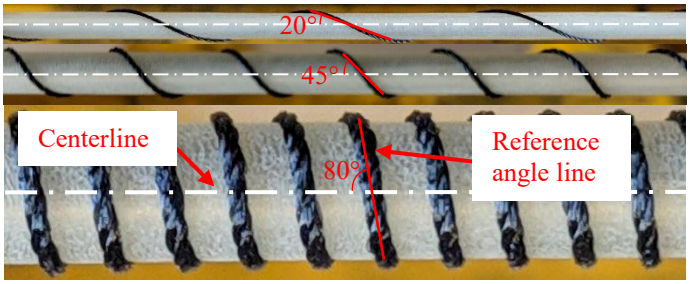

FIGURE 5: 20°, 45° and 80°-degree wrap angles on 2.8mm OD actuator and corresponding overlaid angle reference lines

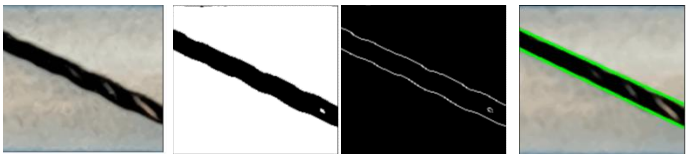

FIGURE 6: Process from initial ROI to angle extraction for the 20° wrap angle. Stages are initial ROI, Binary thresholding in B&W, Canny edge extraction, Hough Transform line and angle extraction: 25°, at average processing duration of 3ms.

3 DISCUSSION

The control scheme presented was adequate for wrapping 10mm and 2.8mm OD actuators (Fig. 7). Startup effects (Table 1) were confined to one end of the actuator and are tolerable since these regions are pushed over a valve and do not inhibit final actuator performance (Fig. 7).

A 95% rise time was chosen instead of a settling time because the PID controller produced no overshoot for any wrap angle. Rise time was also chosen because the controller was found to not settle to within 2% of the setpoint for the 20° wrap angle during the 10-second trials. The controller did settle to within 2% of the setpoints for 45° and 80° wrap angles. This will be

corrected in future work, possibly by tuning the controller at 20° and 80°.

Qualitatively, the accuracy of the deposited fibers seemed highest for the highest wrap angle (80º, Fig. 5 bottom) and worst for the smallest wrap angle (20º, Fig. 5 top). Computer vision (Fig. 6) supported this observation quantitatively with a 5º discrepancy between desired and actual deposition for 20º wrap angle. It was unclear whether this perceived wrap angle error was due to inaccuracy in the control of motion, deposition, the thread sliding up the catheter after deposition, or was an optical effect resulting from projecting a 3D object (the fiber) onto a 2D plane (reference angle line) for the vision system.

The amplitude-modulated oscillation about the 20º wrap angle setpoint was likely due to non-concentricity in both the small upper and large lower MXL pulleys used in the manufacturing setup (Fig. 2). As each completed a full rotation, the tension in the belt (and as a result, the resistance felt by the motor) oscillated sinusoidally. This can be seen in the high-frequency oscillations on the 20-degree wrap angle line (from the small pulley) and the modulated amplitude of those high-frequency oscillations (from the large pulley). This hypothesis is supported by the increased frequency of these oscillations in the 45º wrap angle line in Figure 4. The same oscillations are present in the 80° wrap angle line but are much smaller in amplitude because of the higher rotational inertia in the system at that wrap angle (v_{rot} of 25.52 mm/s, as opposed to 4.5 and 1.64 mm/s for 45° and 20°, respectively). These velocity oscillations at low wrap angles may be corrected through more tuning of the PID controller and will be further investigated.

The 3ms delay from computer vision suggests online angle analysis is feasible. This will also be further investigated in future work on closed-loop deposition and control of fiber wrap angles. This would allow wrap angles to be varied dynamically, enabling more complex final geometries.

4 CONCLUSION

An automated method for programmable manufacturing of unique (possibly patient-specific) catheter robots was presented. The implemented velocity controller was found to settle between 1.4 and 3.3 seconds, depending on wrap angle. This produced accurate wrap angles for all but the first 6 to 15 mm of the actuator length. Custom 2.8mm and 10mm OD catheter actuators were successfully manufactured (Fig. 7). With 3ms latency, computer vision angle extraction for online control appears to be feasible. Further work will explore this online computer vision angle tracking and varying wrap angle as a function of length.

ACKNOWLEDGEMENTS

Portions of this work were supported by NSF Grant No. 1830950 and the University of Minnesota Undergraduate Research Opportunity Program (UROP).

REFERENCES

[1] Centers for Disease Control and Prevention. (2017). Heart Disease. Information Retrieved from https://www.cdc.gov/heartdisease/facts.htm

[2] Mark D Gilbertson, Gillian McDonald, Gabriel Korinek, James D Van de Ven, and Timothy M Kowalewski. Serially actuated locomotion for soft robots in tube-like environments. IEEE Robotics and Automation Letters, 2(2):1140--1147, 201

[3] J. Bishop-Moser and S. Kota, "Design and modeling of generalized fiber-reinforced pneumatic soft actuators," IEEE Trans. Robot., vol. 31, no. 3, pp. 536–545, Jun. 2015.

[4] Bentley TG, Effros RM, Palar K, Keeler EB. Waste in the U.S. Health care system: a conceptual framework. Milbank Q. 2008;86(4):629-59.

[5] Amirshahi, S., Hayn-Leichsenring, G., Denzler, J., & Redies, C. (2014). Evaluating the Rule of Thirds in Photographs and Paintings, Art & Perception, 2(1-2), 163-182. doi: https://doi.org/10.1163/22134913-00002024

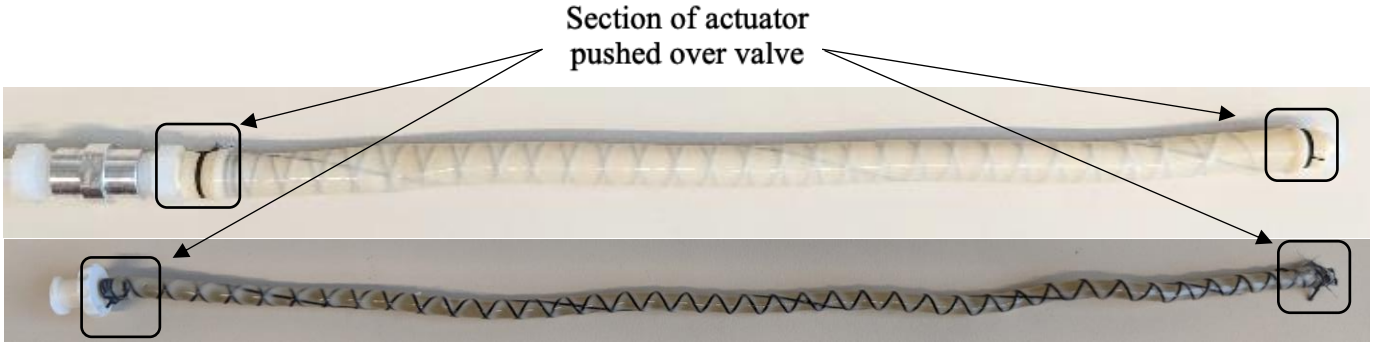

FIGURE 7: Example of two actuators (top OD = 10.8mm, bottom OD = 2.8mm) manufactured on the custom platform each with three different thread fibers deposited at unique wrap angles followed by a dip-cast polyurethane overcoat (Polytek Elastomers, Polytek 74 Series Polyurethane).